EXPLICITLY SOLVABLE KIRCHHOFF AND RIABOUCHINSKY MODELS WITH SEMIPERMEABLE OBSTACLES AND THEIR APPLICATION TO EFFICIENCY ESTIMATION OF FREE FLOW TURBINES

V.M. Silantyev
Northeastern University, Boston MA, USA
e-mail: v.silantyev@neu.edu

В данной работе классические схемы обтекания Кирхгофа и Рябушинского обобщены на случай полупроницаемых препятствий. Рассмотрение данных схем обтекания полупроницаемых препятствий было мотивировано прикладной проблемой теоретической оценки КПД недавно разработанных гидравлических турбин свободного потока.

Introduction

In order to develop potentially huge alternative hydropower resourses, such as ocean currents, tidal streams, low-grade rivers, etc. where construction of dams can be very expensive or even impossible, engineers have been working on hydraulic turbines that can operate in free (non-ducted) flows. The turbines of these kind can be used for harnessing energy from alternative "clean" resources, like ocean currents or tidal streams, without harming the environment or causing a potential risk for the surrounding area in the case of emergency or deliberate damage.

Conventional turbines whose efficiency in ducted flows sometimes can be close to 90 % usually show very poor performance in the free flow applications. The reason for this is that their design allows them to utilize effectively only the potential component of the flow at the expence of the kinetic one. Therefore high efficiency can achieved by increasing the solidity of a turbine that builds up the water head and makes the kinetic component negligibly small. In the free flow case the situation is completely reversed because the kinetic part dominates and therefore requires entirely different technological solitions. Since the beginning of the century, a number of propeller-type turbines has been designed specifically for free flows, but their efficiency did not exceed 18–20 % in practical tests [1 – 3]. In 1931 Darrieus (France) patented a barrell shaped cross-flow turbine with three straight blades, which demonstrated 23.5 % effiency [1, 3]. This turbine however has not received broad practical application mostly due to the pulsations in its rotation leading to the earlier fatigue failure of its parts and also the self-starting problem. In the brand new Gorlov turbine (1998) both these defects are eliminated by using helical (spiral) arrangement of the blades that also increases the efficiency up to 35 % making it ready for commercial use [1]. Nethertheless, since in the free flow case some part of the stream always has the possibility to escape, the efficiency may not be as high as it is in the case of ducted flow. Therefore the problem of theoretical estimate of the efficiency attains its fundamental importance for the further development of free flow turbines. In addition, a theoretical model proposed for this purpose may allow us to compare the parameters of actual turbines with the corresponding theoretically optimal values in order to set up the guidelines for their future improvement.

The first important question in the investigation of the free flow efficiency problem can be posed disregarding the specific construction of the actual turbine. Namely, the turbine, or more generally, the entire section of turbines can be substituted by partially penetrable obstacle absorbing energy from the flow which passes through it. Clearly, in the free flow case the increase of the resistance of the obstacle, which is needed for better use of the energy of the passing through flow, forces more water to streamline it that can eventually result in the loss of net efficiency. Thus the resistance has to be optimized to obtain maximal efficiency and the optimal fraction of the flow that goes through the turbine. For an actual device, both these parameters can be measured experimentally and compared with the theoretical optimum.

In the first approximation water can be substituted by ideal inviscid incompressible liquid, but the well-known d'Alembert paradox implies that the drag on the obstacle which force the flow to get in is zero if the current streamlines the obstacle completely without separation. This problem can be avoided by considering a Helmholtz-type wake flow. The basic examples of flows of this type are the Kirchhoff and Riabouchinsky models which are shown in Fig. 1.

Both these classical situations consider the direct impact of the stream on an impervious lamina placed perpendicular to it. The flow separates from the edges forming the stagnation domain past the lamina. In the Kirchhoff model (Fig. 1, *a*) the separating streamlines γ and γ' are determined from the condition that the pressure inside the stagnation domain is the same as the pressure at infinity that implies that the velocity V_γ on the separating streamlines is the same as the velocity at infinity. However, under this condition the stagnation domain past the obstacle becomes infinite. In the Riabouchinsky model this problem is avoided by placing the virtual obstacle behind the actual one (Fig. 1, *b*), where the separating streamlines join the

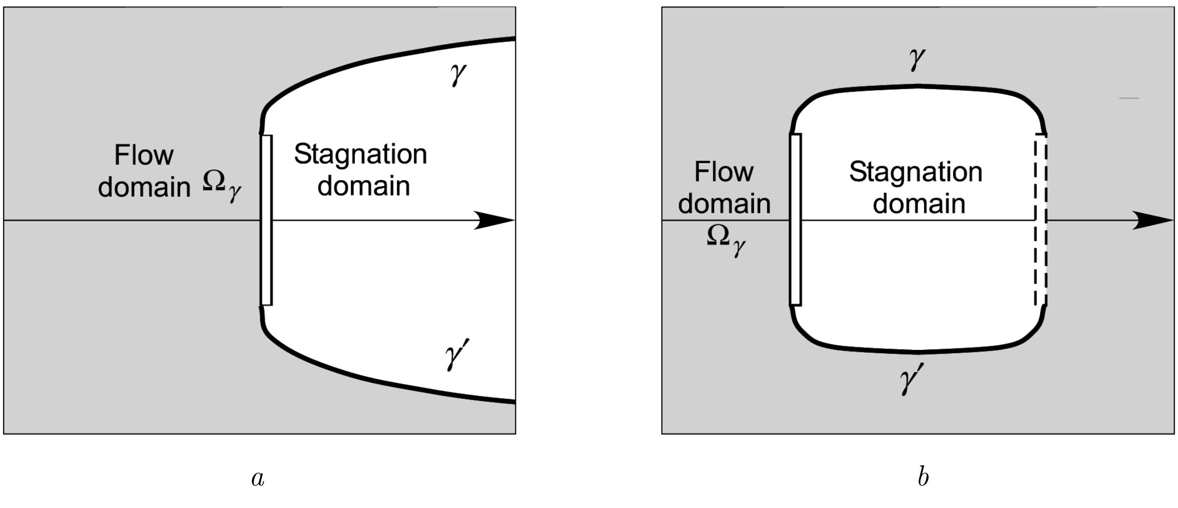

Fig. 1. Kirchhoff and Riabouchinsky models: *a* — Kirchhoff model; *b* — Riabouchinsky model.

edges of both laminae making the stagnation domain finite. In this situation the pressure in the stagnation domain is actually lower then one at infinity therefore the velocity V_γ on the streamlines γ and γ' is greater that the velocity at infinity V_∞. The number σ such that

$$1 + \sigma = \frac{V_\gamma^2}{V_\infty^2} \tag{1}$$

is called *cavitation number*. The important advantage of the Riabouchinsky model is its capability to deal with variably small cavitation numbers.

In this paper both these models will be generalized for the case of partially penetrable obstacles. It will be shown that under some additional assumptions they both have explicitly solvable situations and the solution can be constructed by means of the Kirchhoff transform similarly to the classical case. For a partially penetrable obstacle, its "efficiency" can be naturally defined as the ratio of the absorbed power P to the power P_∞ carried by undisturbed flow through the projected area of the obstacle perpendicular to the stream. It turns out that the numerical evaluation of this efficiency obtained from these models is in a reasonable agreement with the practical tests [2].

1. Complex variable methods in two-dimensional problems of hydrodynamics: main defininitions and brief review

Many two dimensional problems of hydrodynamics of ideal inviscid incompressible fluid can be effectively treated using complex variable methods. Let (x, y) be the coordinates in the two-dimensional real affine space $\mathbb{R}^2$, which is identified with one-dimensional complex space $\mathbb{C}$ by taking $z = x + iy$. All vectors and vector field will be also identified with complex numbers and complex variable functions respectively. Consider a steady flow of this fluid in a certian domain $\Omega \subset \mathbb{R}^2$. Its velocity field $\mathbf{V}$ satisfies the continuity equation

$$\nabla \cdot \mathbf{V} = 0 \tag{2}$$

in Ω. Assume that Ω is connected and fix a certain point $P_0 \in \Omega$. For an arbitrary point $P \in \Omega$ consider the flux of $\mathbf{V}$ through a certain C^1-smooth path ω connecting P and P_0 given by

$$v = \int_\omega -V_y\, dx + V_x\, dy. \tag{3}$$

By virtue of (2) the form $-V_y\, dx + V_x\, dy$ is closed, therefore the flux doesn't depend on the choice of ω within the same homotopy class. If Ω is simply connected, then $v(P)$ is well-defined in Ω and it is called the stream function of the flow. If in addition the flow is irrotational, i.e.

$$\nabla \times \mathbf{V} = \left(\frac{\partial V_y}{\partial x} - \frac{\partial V_x}{\partial y} \right) = 0 \tag{4}$$

the stream function v is harmonic since

$$\Delta v = \frac{\partial^2 v}{\partial x^2} + \frac{\partial^2 v}{\partial y^2} = -\frac{\partial V_y}{\partial x} + \frac{\partial V_x}{\partial y} = 0. \tag{5}$$

Let u denote a harmonically conjugate function to v, s.t. $w = u + iv$ is holomorphic in Ω. Then it's easy to check that

$$\mathbf{V} = \nabla u = \overline{\frac{dw}{dz}} \tag{6}$$

and the functions u and w are called the real and the complex potentials of the flow respectively. The important property of the potential w is that it straightens the streamlines when it is considered as a conformal map of the flow domain Ω. Therefore, the problem of finding the velocity field of the flow can be reduced to the problem of finding conformal representation of some specified domains. The diagrams illustrating this process are called Agrand diagrams [4].

2. The classical Kirchhoff model with an impervious lamina

As mentioned in the introduction, the Kirchhoff model describes a direct impact of the stream on a lamina which is impervious in the classical situation. Its Agrand diagram is presented in Fig. 2. The stream separates from the edges of the lamina and the separating streamlines γ and

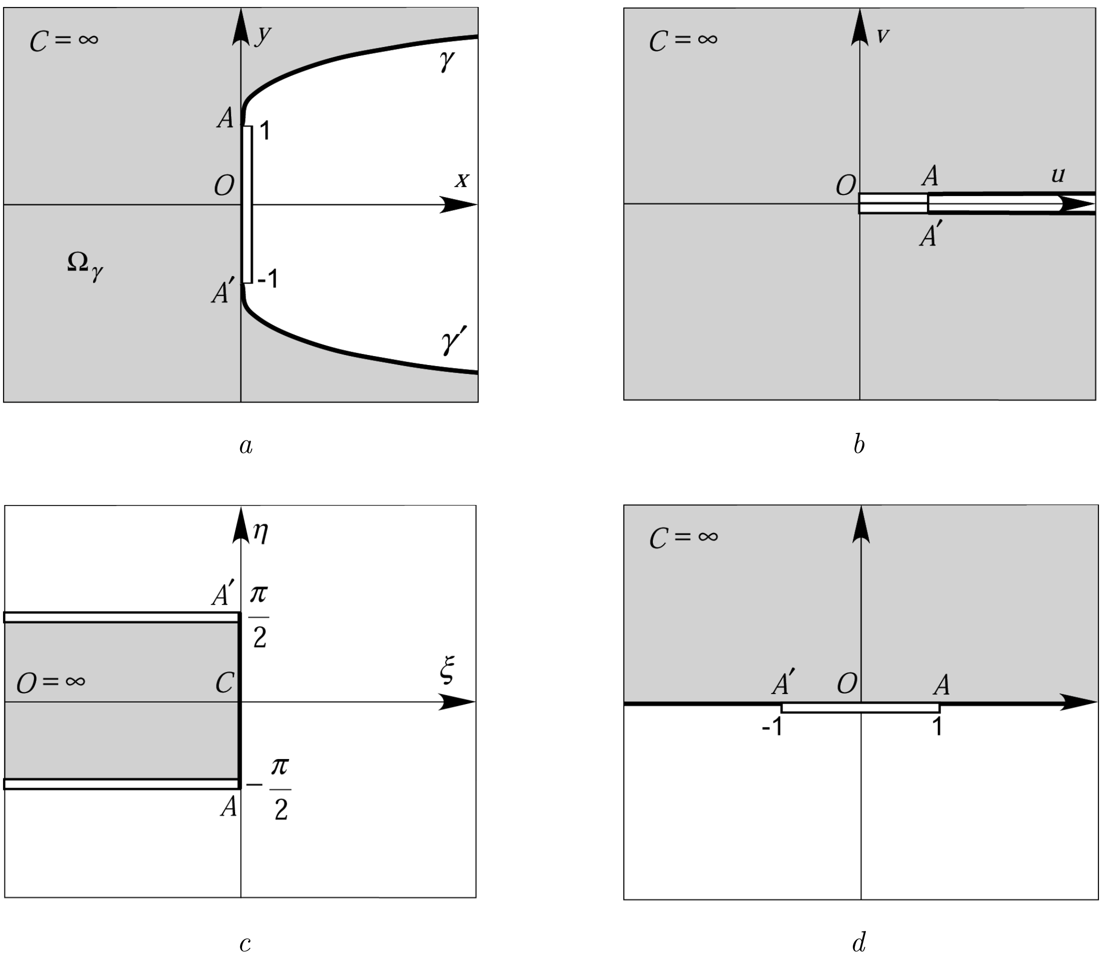

Fig. 2. Classical Kirchhoff flow with an impervious lamina: a — z-plane; b — potential w-plane; c — hodograph ζ-plane; d — t-plane.

γ' are a priori unknown. They are determined from the Kirchhoff condition that the pressure in the stagnation domain $\mathbb{C} \setminus \Omega_\gamma$ is the same as the pressure at infinity. This condition implies that

$$V = V_\infty \tag{7}$$

holds on both separating streamlines γ and γ'. For the sake of convenience, the units of mass, distance, and time can be scaled in such a way that the velocity of the stream at infinity V_∞, the half of the length of the lamina l and the density of the liquid are all equal to 1 by taking

$$\mathbf{V} = \frac{1}{V_\infty}\mathbf{V}_{\text{actual}}, \quad x = \frac{x_{\text{actual}}}{l}, \quad y = \frac{y_{\text{actual}}}{l}, \quad \rho = 1. \tag{8}$$

It follows directly from the definition that the conformal mapping $w(z)$ rectifies all streamlines making them parallel to u-axis [4, 5]. In the classical situation of an impervious lamina, there is no gap between the separating streamlines. Hence $w(z)$ maps the flow domain Ω_γ onto the complement to the positive u-axis (Fig. 2, b).

3. Hodograph Variable

Up to now the condition (7) has not been reflected in the Agrand diagram for the potential w. However its geometric meaning becomes clear in the *hodograph plane* defined by

$$\zeta = \xi + i\eta = \log\frac{\partial w}{\partial z}, \quad \xi = \log V, \quad \eta = -\arg w.$$

It's easy to verify that that the image of the flow domain of Ω_γ is the semi-strip

$$S_0 = \left\{(\xi,\eta): \ -\infty < \xi < 0, \ -\frac{\pi}{2} < \eta < \frac{\pi}{2}\right\}$$

as shown in Fig. 2, c. The condition (7) implies that the images of the free streamlines on this hodograph plane lie on the ξ-axis. This completes the setup of the free boundary problem in terms of the Agrand diagram. The same problem can be alternatively formulated using real potential u

$$\begin{aligned}
\Delta u &= 0 \quad \text{in } \Omega_\gamma;\\
\frac{\partial u}{\partial \boldsymbol{\nu}} &= 0 \quad \text{on} \quad \{(x,y): \quad x = 0, \ -1 \le y \le 1\};\\
\frac{\partial u}{\partial \boldsymbol{\nu}} &= 0 \quad \text{on } \gamma \text{ and } \gamma' \text{ (since they both are streamlines)};\\
\frac{\partial u}{\partial \boldsymbol{\tau}} &= 1 \quad \text{on } \gamma \text{ (constant velocity condition)};\\
\frac{\partial u}{\partial \boldsymbol{\tau}} &= -1 \quad \text{on } \gamma' \text{ (constant velocity condition)};\\
u(0) &= 0
\end{aligned}$$

or the stream function v

$$\begin{aligned}
\Delta v &= 0 \quad \text{in } \Omega_\gamma;\\
\frac{\partial v}{\partial \boldsymbol{\tau}} &= 0 \quad \text{on} \quad \{(x,y): \quad x=0,\ -1\le y\le 1\};\\
\frac{\partial v}{\partial \boldsymbol{\tau}} &= 0 \quad \text{on } \gamma \text{ and } \gamma' \text{ (since they both are streamlines)};\\
\frac{\partial v}{\partial \boldsymbol{\nu}} &= 1 \quad \text{on } \gamma \text{ (constant velocity condition)};\\
\frac{\partial v}{\partial \boldsymbol{\nu}} &= -1 \quad \text{on } \gamma' \text{ (constant velocity condition)};\\
v(0) &= 0,
\end{aligned}$$

where $\boldsymbol{\nu}$ is the outward normal and $\boldsymbol{\tau} = i\boldsymbol{\nu}$ is the tangent vector. However the conformal mapping setup has a crucial advantage versus the setups described above, that will be explained in the next section.

4. The Kirchhoff method

A remarkable fact is that the Agrand diagram not only makes the setup of the problem more comprehensive, but also provides the clue to its solution. Namely, the problem stated in two previous sections is well-posed and can be solved by the Kirchhoff method (see [4]).

The idea of this method is to obtain the differential equation for the conformal representation of the flow domain (which contains free boundaries) using the conformal representations of its images on w- and ζ-plains whose boundaries are known up to some finite numbers of parameters and the fact that $\zeta = \log \dfrac{\partial w}{\partial z}$. Let the upper semi-plane be the canonical domain parametrized by variable t (Fig. 2, *d*). Then the conformal representation of the semi-strip on ζ-plane with the boundary extension as shown in Fig. 2, *c* is given by

$$\zeta = -\log\left(\frac{1}{t} + \frac{1}{t}\sqrt{1-t^2}\right) - i\frac{\pi}{2}.$$

The conformal representation of the image of Ω_γ on w-plane is as follows

$$w = \frac{1}{2}Kt^2, \quad \frac{dw}{dt} = Kt,$$

where K is a positive real constant to be determined. Then

$$\begin{aligned}
-\zeta &= \log\frac{dz}{dw} = \log\left(\frac{1}{t} + \frac{1}{t}\sqrt{1-t^2}\right) + \frac{i\pi}{2};\\
\frac{dz}{dw} &= \frac{i}{t}\left(1+\sqrt{1-t^2}\right);\\
\frac{dz}{dt} &= \frac{dz}{dw}\frac{dw}{dt} = iK\left(1+\sqrt{1-t^2}\right).
\end{aligned}$$

The constant K can be found from the condition $i = \int_0^1 \frac{dz}{idt}\, dt$ as follows

$$\begin{aligned} i &= iK \int_0^1 \left(1 + \sqrt{1-t^2}\right)\, dt = iK\left(1 + \frac{\pi}{4}\right), \\ K &= \frac{1}{1 + \frac{\pi}{4}} = \frac{4}{4+\pi}. \end{aligned}$$

Hence the desired conformal representation of Ω_γ is given by the formula

$$z(t) = \frac{4}{4+\pi} \int_0^t \left(1 + \sqrt{1-\tau^2}\right)\, d\tau$$

that solves the problem in the sense that it allows us to find the free boundaries and the drag on the lamina.

5. The drag in the classical Kirchhoff model

The drag D on the lamina can be computed as the integral of the pressure drop $[p]$ across the lamina

$$\begin{aligned} D &= \int_{-l}^{l} [p_{\text{actual}}]\, dy = \frac{lV_\infty^2}{2} \int_{-1}^{1} \left(1 - V^2\right)\, dy = \\ &= lV_\infty^2 \int_0^1 \left(1 - \left|\frac{dw}{dz}\right|^2\right) \frac{dz}{idt}\, dt = \\ &= lV_\infty^2 \left(1 - K \int_0^1 \left(\frac{t}{1+\sqrt{1-t^2}}\right)^2 \left(1 + \sqrt{1-t^2}\right)\, dt\right) = \\ &= lV_\infty^2 \left(1 - K \int_0^1 \left(1 - \sqrt{1-t^2}\right)\, dt\right) = \\ &= lV_\infty^2 \left(1 - \frac{4}{\pi+4}\left(1 - \frac{\pi}{4}\right)\right) = \\ &= lV_\infty^2 \left(1 - \frac{4-\pi}{4+\pi}\right) = \frac{2\pi}{\pi+4} lV_\infty^2. \end{aligned}$$

The number $\frac{2\pi}{\pi+4} \approx 0.88$ is called the *drag coefficient* (see [4]).

6. The modified Kirchhoff model with a partially penetrable lamina

The classical Kirchhoff model described above can be generalized for the case of a partially penetrable lamina whose permeability may vary along the lamina. This generic situation can hardly be explicitly solvable, however if one assumes that *all streamlines cross the lamina at the same angle at any point* (up to the symmetry) then the explicit solution exists and can be constructed in a similar way. The Agrand diagram of this modified Kirchhoff model is presented in Fig. 3. Since some part of the flow goes through the lamina there is a gap between the images of the separating streamlines. Denote half of the width of the gap by s (see Fig. 3, b). In the system of units introduced in (8), the velocity of the flow at infinity equals 1; that means that the potential map $w(z)$ tends to the identity map as $|z| \to \infty$. Therefore the distance between the separating streamlines in the z-plane tends to $2s$ as $x \to -\infty$. In other words s can be also interpreted as the fraction of the flow that passes through the obstacle.

In order to apply the Kirchhoff method we first construct the conformal representation of the semi-strip

$$S_1 = \{(\xi, \eta) : \infty < \xi < 0, \quad -\frac{\pi}{2} + \alpha < \eta < \frac{\pi}{2} - \alpha\}$$

on ζ-plane. In this case the width of the semi-strip is equal to $2 - \dfrac{4\alpha}{\pi}$, since the current crosses

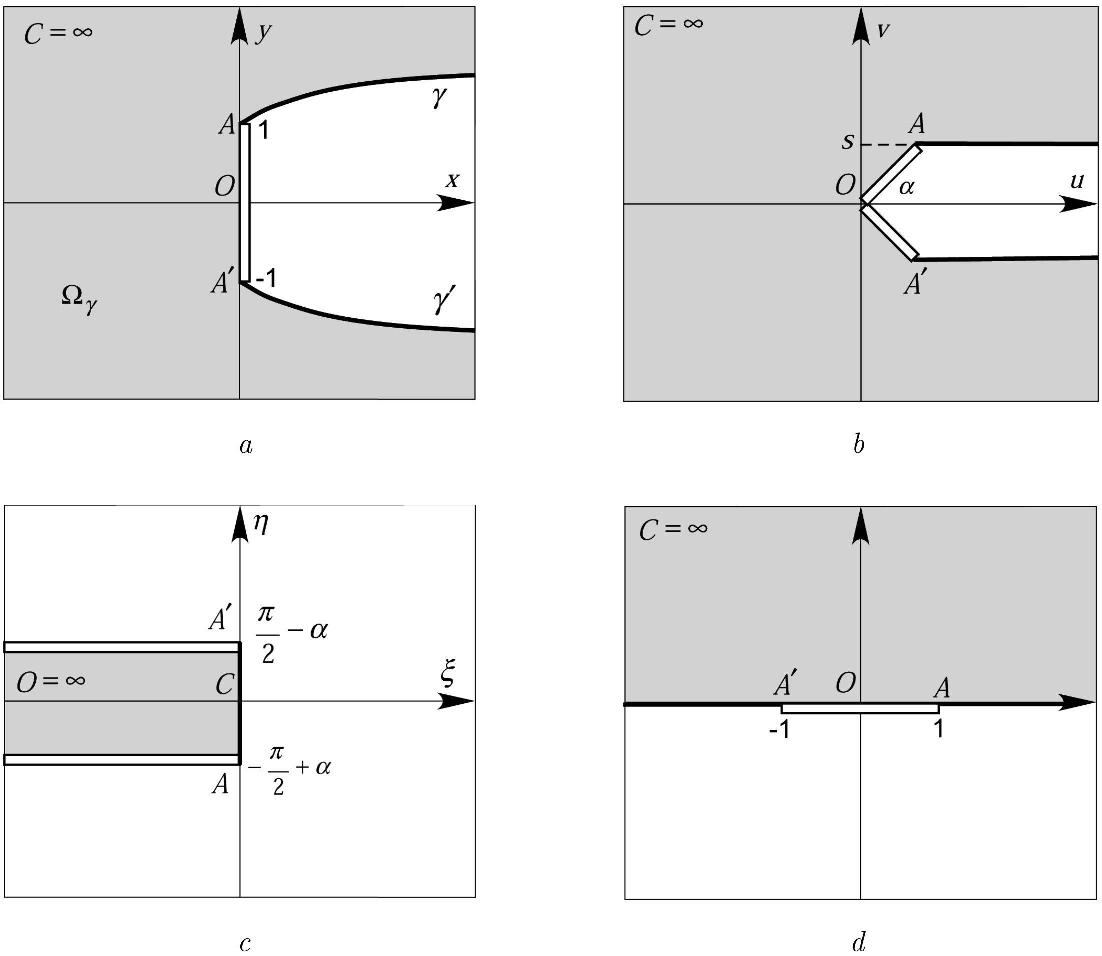

Fig. 3. Modified Kirchhoff flow with a partially penetrable lamina: a — z-plane; b — potential w-plane; c — hodograph ζ-plane; d — t-plane.

the lamina at an angle α (Fig. 3, c). Therefore it is given by

$$\zeta = -\left(1 - \frac{2\alpha}{\pi}\right) \log\left(\frac{1}{t} + \frac{1}{t}\sqrt{1-t^2}\right) - i\left(\frac{\pi}{2} - \alpha\right).$$

The conformal representation of the image of the flow domain Ω_γ on w-plane is constructed using the Christoffel — Schwarz integral

$$\begin{aligned} \frac{dw}{dt} &= \frac{2s}{\alpha}\left(t^2-1\right)^{\frac{\alpha}{\pi}} t^{\left(1-\frac{2\alpha}{\pi}\right)}, \\ w(t) &= \frac{2s}{\alpha}\int_0^t \left(\tau^2-1\right)^{\frac{\alpha}{\pi}} \tau^{\left(1-\frac{2\alpha}{\pi}\right)}\, d\tau. \end{aligned}$$

Then

$$\begin{aligned} \log\frac{dz}{dw} &= \left(1-\frac{2\alpha}{\pi}\right)\log\left(\frac{1}{t}+\frac{1}{t}\sqrt{1-t^2}\right) + i\left(\frac{\pi}{2}-\alpha\right), \\ \frac{dz}{dw} &= e^{i\left(\frac{\pi}{2}-\alpha\right)}\left(1+\sqrt{1-t^2}\right)^{1-\frac{2\alpha}{\pi}} t^{\frac{2\alpha}{\pi}-1}, \\ \frac{dz}{dt} &= \frac{dz}{dw}\cdot\frac{dw}{dt} = \frac{2is}{\alpha}\left(1+\sqrt{1-t^2}\right)^{1-\frac{2\alpha}{\pi}}\left(1-t^2\right)^{\frac{\alpha}{\pi}}. \end{aligned}$$

Since $\int_0^1 \frac{dz}{dt}\,dt = i$, then

$$s = \frac{\alpha}{2I_2},$$

where

$$I_2 = \int_0^1 \left(1+\sqrt{1-t^2}\right)^{1-\frac{2\alpha}{\pi}}\left(1-t^2\right)^{\frac{\alpha}{\pi}}\, dt.$$

The formula

$$z(t) = \frac{i}{I_2}\int_0^t \left(1+\sqrt{1-\tau^2}\right)^{1-\frac{2\alpha}{\pi}}\left(1-\tau^2\right)\, d\tau$$

provides the conformal representation of the flow domain Ω_γ which solves the free boundary problem in the same sense as in the classical situation.

7. The efficiency in the modified Kirchhoff model

The modified Kirchhoff flow with a partially penetrable lamina studied in the previous sections can be an approximate model of a free flow turbine or the entire section of many turbines. The absorbed power can be computed as the integral over the lamina of the pressure drop $[p]$ across it multiplied by the x-component of the velocity

$$P = \int_{-1}^{1} [p] V_x\, dy.$$

The power carried by the undisturbed flow through the lamina of width 2 is

$$P_\infty = 2\frac{\rho V_\infty^3}{2} = 1.$$

The efficiency can be naturally defined as their ratio

$$\mathcal{E} = \frac{P}{P_\infty} \tag{9}$$

(Since the efficiency is dimensionless we can use the system of units introduced in (8) in which ρ and V_∞ are both equal to 1). By virtue of the Bernoulli theorem $[p] = \dfrac{V_\infty^2 - V^2}{2} = \dfrac{1 - V^2}{2}$ and

Table 1

No	Inclination angle, α	Efficiency, $\mathcal{E}$	Flow through, s
0	0.00000	0.00000	0.00000
1	0.07854	0.01761	0.02294
2	0.15708	0.03646	0.04785
3	0.23562	0.06922	0.09168
4	0.31416	0.07771	0.10405
5	0.39270	0.09998	0.13559
6	0.47124	0.12320	0.16961
7	0.54978	0.14717	0.20623
8	0.62832	0.17164	0.24562
9	0.70686	0.19625	0.28793
10	0.78540	0.22050	0.33333
11	0.86394	0.24371	0.38199
12	0.94248	0.26494	0.43409
13	1.02102	0.28292	0.48983
14	1.09956	0.29582	0.54940
15	1.17810	0.30113	0.61302
16	1.25664	0.29521	0.68091
17	1.33518	0.27274	0.75331
18	1.41372	0.22569	0.83044
19	1.49226	0.14158	0.91259
20	1.57080	0.00000	1.00000

$$\begin{aligned}
\mathcal{E} &= \frac{P}{P_\infty} = \frac{1}{2}\int\limits_{-1}^{1} V_x\left(1-V^2\right)\,dy = \int\limits_{0}^{1} V_x\left(1-V^2\right)\,dy = \\
&= \int\limits_{0}^{1}\left(\mathrm{Re}\frac{dw}{dz}\right)\left(1-\left|\frac{dw}{dz}\right|^2\right)dy = \frac{1}{i}\int\limits_{0}^{1}\left(\mathrm{Re}\frac{dw}{dz}\right)\left(1-\left|\frac{dw}{dz}\right|^2\right)\frac{dz}{dt}dt = \\
&= s-\frac{1}{i}\int\limits_{0}^{1}\left(\mathrm{Re}\frac{dw}{dz}\right)\left|\frac{dw}{dz}\right|^2\frac{dz}{dt}dt = \\
&= s-\sin\alpha\int\limits_{0}^{1}\left|\frac{dw}{dz}\right|^3\frac{dz}{i\,dt}dt = \frac{1}{I_2}\left(\frac{\alpha}{2}-I_3\sin\alpha\right),
\end{aligned}$$

where

$$I_3 = \frac{I_2(\alpha)}{i}\int\limits_{0}^{1}\left|\frac{dw}{dz}\right|^3\frac{dz}{dt}dt = \int\limits_{0}^{1}\left(1+\sqrt{1-t^2}\right)^{\frac{4\alpha}{\pi}-2}\left(1-t^2\right)^{\frac{\alpha}{\pi}}t^{3-\frac{6\alpha}{\pi}}\,dt.$$

The results of numerical evaluation of the efficiency $\mathcal{E}$ and the fraction s of the flow passing through the turbine are presented in Table 1. The inclination angle α ranges from 0 (impervious lamina) to $\frac{\pi}{2}$ (undisturbed flow). The maximum efficiency of 30 % is attained when $\alpha = \frac{3\pi}{8}$ and $s = 0.61$, which means that in free flow the solidity of the optimal turbine should be rather low, unlike in the ducted flow case where high efficiency is achieved by increasing the solidity.

8. The classical Riabouchinsky model with an impervios lamina

The main defect of the classical Kirchhoff model is the infinite size of the stagnation domain resulting from the condition that the pressure past the lamina is the same as the pressure at infinity. In the Riabouchinsky model this defect is eliminated by placing the same *virtual lamina* past the actual one. The separating streamlines γ and γ' connect the edges of both laminae making the stagnation domain bounded (Fig. 1, *b*). The pressure inside the stagnation domain becomes lower than the pressure at infinity, therefore the velocity on the separating streamlines becomes bigger than the velocity at infinity.

Since the picture of the flow is symmetric with respect to the vertical line in the middle between the actual and the virtual laminae (with reverting of the direction of the flow), it suffices to consider only one (the left) part of the flow. Its Agrand diagram is presented in Fig. 4.

This model can be also treated by the same Kirchhoff method, but the computations become slightly more complicated. The image of the stagnation domain Ω_γ in this case is a semistrip with a cut along the positive x-axis

$$S_0' = \{(\xi,\eta):\ -\infty < \xi < \log V_\gamma,\ -\frac{\pi}{2} < \eta < \frac{\pi}{2}\} \setminus \{(\xi,\eta):\ \xi > 0, \eta = 0\}.$$

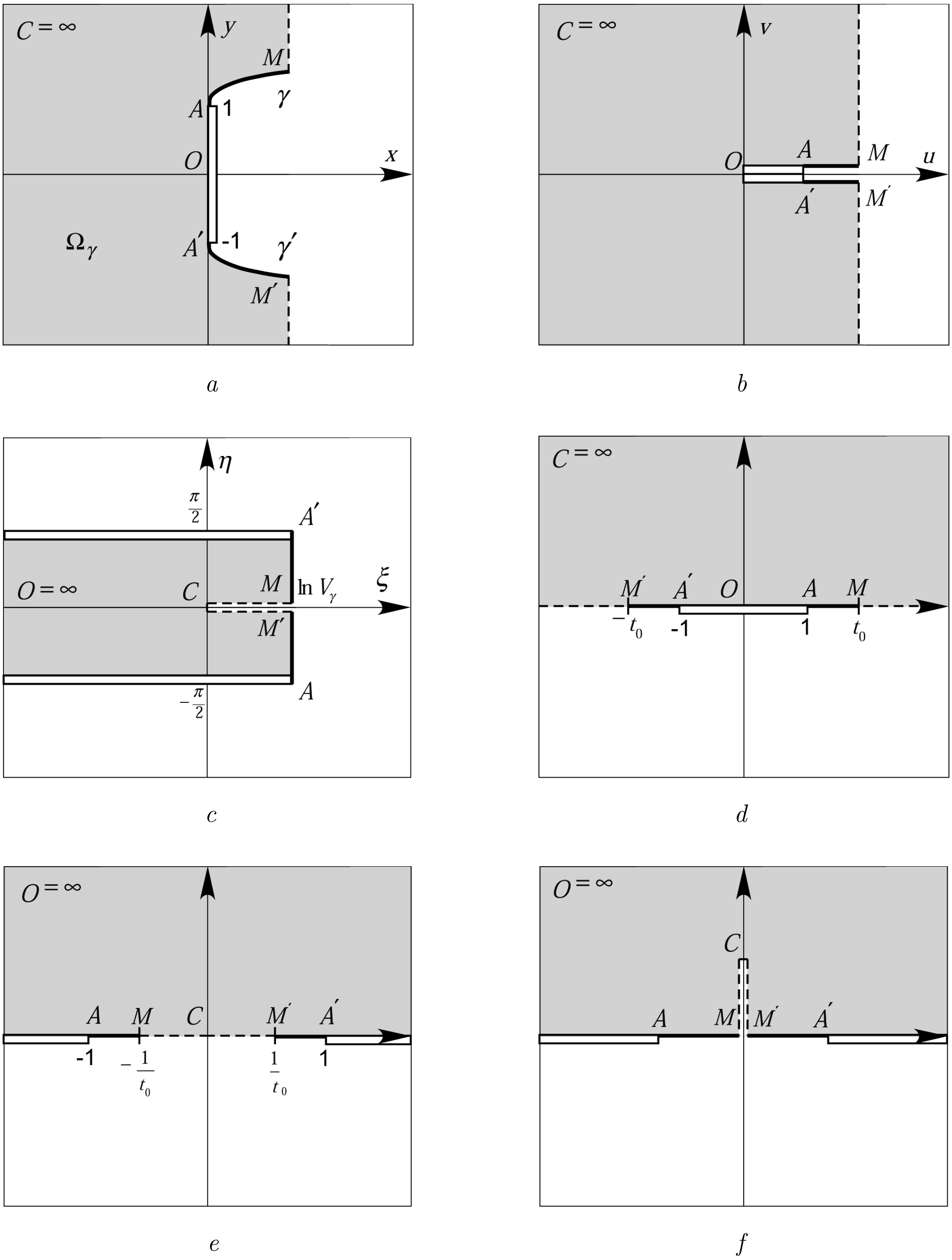

Fig. 4. Classical Riabouchinsky flow with an impervious lamina: a — z-plane; b — potential w-plane; c — hodograph ζ-plane; d — t-plane; e — T-plane; f — a-plane.

Its conformal representation is constructed in two steps using auxiliary variables

$$T = -\frac{1}{t},$$

and

$$a = \sqrt{\frac{T^2 - \frac{1}{t_0^2}}{1 - \frac{1}{t_0^2}}} = \frac{1}{t}\sqrt{\frac{t_0^2 - t^2}{t_0^2 - 1}}.$$

Then

$$\begin{aligned} \zeta &= -\log\left(a + \sqrt{a^2 - 1}\right) - i\frac{\pi}{2} + \log V_\gamma = \\ &= -\log\left(\frac{1}{t}\sqrt{\frac{t_0^2 - t^2}{t_0^2 - 1}} + \frac{t_0}{t}\sqrt{\frac{1 - t^2}{t_0^2 - 1}}\right) - i\frac{\pi}{2} + \log V_\gamma, \end{aligned}$$

where t_0 is undetermined up to now. Since the point $C = \infty$ on the t-plane maps to the origin on the hodograph plane

$$\begin{aligned} -\log V_\gamma &= -\log\left(\sqrt{\frac{-1}{t_0^2 - 1}} + t_0\sqrt{\frac{-1}{t_0^2 - 1}}\right) - \frac{i\pi}{2}, \\ V_\gamma &= \sqrt{\frac{t_0 + 1}{t_0 - 1}}. \end{aligned}$$

The last equality yields the relation between the cavitation number σ and the parameter t_0:

$$1 + \sigma = V_\gamma^2 = \frac{t_0 + 1}{t_0 - 1}.$$

The conformal representation of the image of Ω in the potential w-plane is still constructed using the Christoffel — Schwarz integral

$$\begin{aligned} \frac{dw}{dt} &= \frac{iKt}{\sqrt{t^2 - t_0^2}}, \\ w &= iK\int_0^t \frac{\tau\, d\tau}{\sqrt{\tau^2 - t_0^2}}, \end{aligned}$$

where K is another undetermined constant. Now we can find the conformal representation of Ω_γ using the Kirchhoff method:

$$\begin{aligned} \zeta &= -\log\frac{dz}{dw} = -\log\left(\frac{1}{t}\sqrt{\frac{t_0^2 - t^2}{t_0^2 - 1}} + \frac{t_0}{t}\sqrt{\frac{1 - t^2}{t_0^2 - 1}}\right) - \frac{i\pi}{2} + \log V_\gamma, \\ \frac{dz}{dw} &= \frac{i}{V_\gamma}\left(\frac{1}{t}\sqrt{\frac{t_0^2 - t^2}{t_0^2 - 1}} + \frac{t_0}{t}\sqrt{\frac{1 - t^2}{t_0^2 - 1}}\right), \\ \frac{dz}{dt} &= \frac{dz}{dw}\cdot\frac{dw}{dt} = \frac{iK}{V_\gamma}\left(\sqrt{\frac{t_0^2 - t^2}{t_0^2 - 1}} + t_0\sqrt{\frac{1 - t^2}{t_0^2 - 1}}\right)\frac{1}{\sqrt{t_0^2 - t^2}}, \\ z &= \frac{iK}{V_\gamma\sqrt{t_0^2 - 1}}\left(t + t_0\int_0^t \sqrt{\frac{1 - \tau^2}{t_0^2 - \tau^2}}\, d\tau\right). \end{aligned} \tag{10}$$

The constant K can be found from the condition $\int\limits_0^1 \frac{dz}{idt}dt = 1$ that implies that

$$K = \frac{V_\gamma \sqrt{t_0^2 - 1}}{1 + t_0 \int\limits_0^1 \sqrt{\frac{1-t^2}{t_0^2 - t^2}}\, dt}. \tag{11}$$

The conformal representation of Ω_γ is given by (10) and (11). It may be shown [4] that for small cavitation numbers

$$C_D(\sigma) = (1+\sigma)C_D(0),$$

where $C_D(\sigma)$ denotes the drag coefficient, considered as a function of σ.

9. The modified Riabouchinsky flow with a partially penetrable lamina

In the modified Kirchhoff flow described above the stagnation domain past the lamina is also unbounded. It happens because of the same assumption that the pressure inside the stagnation domain is equal to the pressure at infinity corresponding to the case of zero cavitation number. The more precise modified Riabouchinsky model with a semi-penetrable plane considered in this section allows us to work with variably small cavitation numbers as its classical analog described in Section 8 does. In this model the same virtual lamina is placed past the actual one and the free streamlines γ and γ' join the edges of both laminae as in the classical case (see Fig. 1, *b*) and the velocity V_γ on the free steramlines is determined from the equation (1). As in the case of the modified Kirchhoff model an explicit solution exists under the same assumption that the *inclination angle* α *is the same at any point*. Because of the symmetry of the flow with respect to the middle straight line between the laminae it also suffices to consider the Agrand diagram of the left part of the flow picture, which is presented in Fig. 5.

The solution is constructed using the Kirchhoff method in a way similar to the classical situation. The image of the flow domain Ω_γ on the hodograph plane is the semi-strip

$$S_1' = \{(\xi,\eta) :\ -\infty < \xi < \log V_\gamma,\ -\frac{\pi}{2} + \alpha < \eta < \frac{\pi}{2} - \alpha\} \setminus \{(\xi,\eta) :\ \xi > 0, \eta = 0\}$$

of width $\pi - 2\alpha$ having a cut along positive $\xi =$ axis Fig. 5, *c*. The conformal representation of it is also constructed using the auxiliary variables

$$T = -\frac{1}{t}$$

and

$$\begin{aligned} a &= \frac{1}{t}\sqrt{\frac{t_0^2 - t^2}{t_0^2 - 1}}, \\ \sqrt{a^2 - 1} &= \frac{t_0}{t}\sqrt{\frac{1 - t^2}{t_0^2 - 1}}, \end{aligned}$$

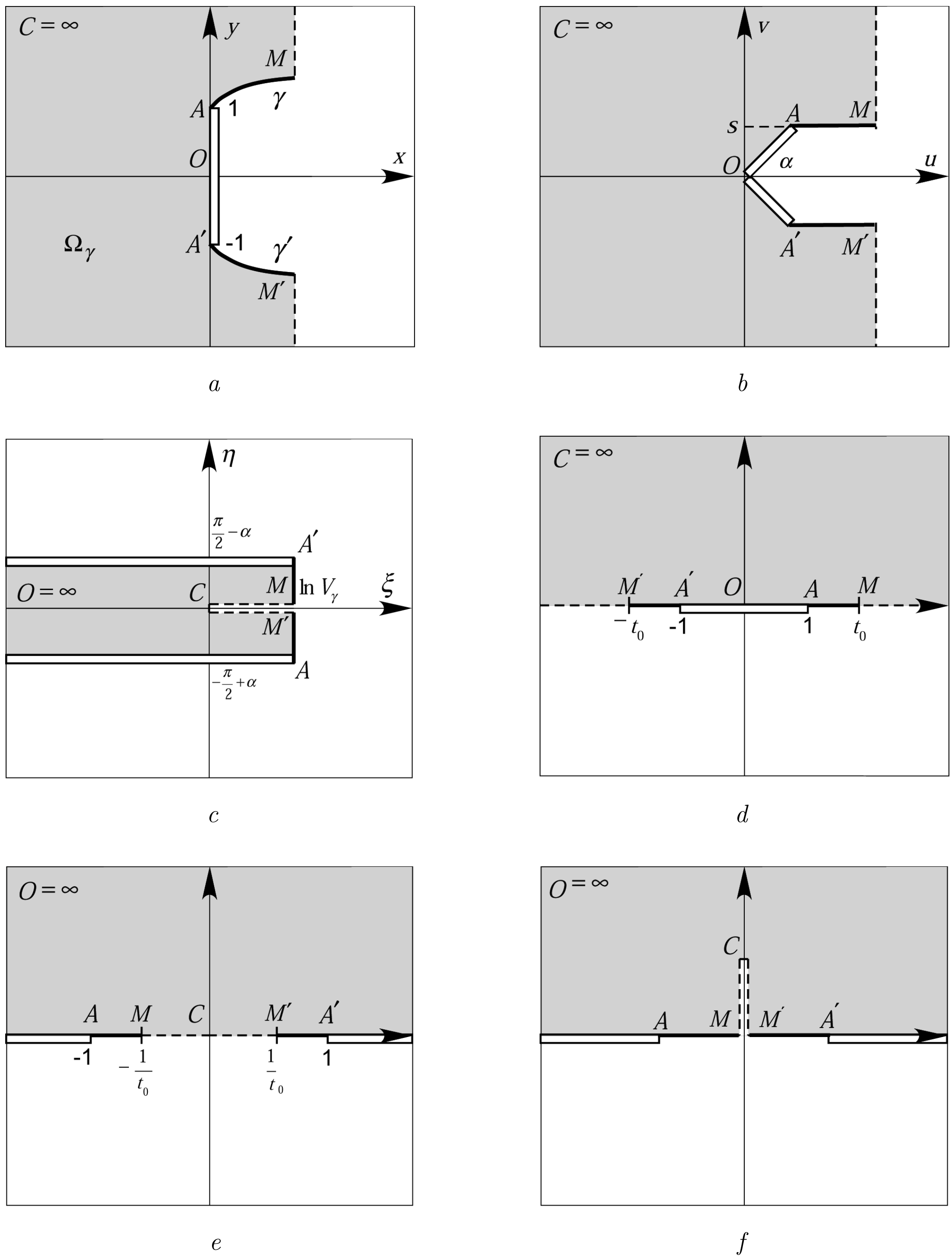

Fig. 5. Modified Riabouchinsky flow with a partially penetrable lamina: a — z-plane; b — potential w-plane; c — hodograph ζ-plane; d — t-plane; e — T-plane; f — a-plane.

as follows

$$\begin{aligned}
\zeta &= -\left(1-\frac{2\alpha}{\pi}\right)\log\left(a+\sqrt{a^2-1}\right)-i\left(\frac{\pi}{2}-\alpha\right)+\log V_\gamma,\\
&= -\left(1-\frac{2\alpha}{\pi}\right)\log\left(\frac{1}{t}\sqrt{\frac{t_0^2-t^2}{t_0^2-1}}+\frac{t_0}{t}\sqrt{\frac{1-t^2}{t_0^2-1}}\right)-i\left(\frac{\pi}{2}-\alpha\right)+\log V_\gamma.
\end{aligned}$$

The point $C=\infty$ maps to the origin, so

$$\begin{aligned}
-\log V_\gamma &= -\left(1-\frac{2\alpha}{\pi}\right)\log\left(\sqrt{\frac{-1}{t_0^2-1}}+t_0\sqrt{\frac{-1}{t_0^2-1}}\right)-i\left(\frac{\pi}{2}-\alpha\right),\\
\log V_\gamma &= \left(1-\frac{2\alpha}{\pi}\right)\log\frac{1+t_0}{\sqrt{t_0^2-1}}=\left(1-\frac{2\alpha}{\pi}\right)\log\sqrt{\frac{t_0+1}{t_0-1}},\\
V_\gamma &= \left(\frac{t_0+1}{t_0-1}\right)^{\frac{1}{2}-\frac{\alpha}{\pi}}.
\end{aligned}$$

The conformal representation of the area on the potential w-plane with the boundary extension as shown in Fig. 5, b is given by

$$\begin{aligned}
\frac{dw}{dt} &= iK\left(t^2-t_0^2\right)^{-\frac{1}{2}}\left(t^2-1\right)^{\frac{\alpha}{\pi}}t^{1-\frac{2\alpha}{\pi}},\\
w &= iK\int_0^1\left(\tau^2-t_0^2\right)^{-\frac{1}{2}}\left(\tau^2-1\right)^{\frac{\alpha}{\pi}}\tau^{1-\frac{2\alpha}{\pi}}\,d\tau.
\end{aligned}$$

The fraction s of the flow passing through the turbine is determined from

$$\begin{aligned}
\frac{se^{i\alpha}}{\sin\alpha} &= iK\int_0^1\left(\tau^2-1\right)^{\frac{\alpha}{\pi}}\left(\tau^2-t_0^2\right)^{-\frac{1}{2}}\tau^{1-\frac{2\alpha}{\pi}}\,d\tau,\\
s &= KI_4\sin(\alpha),
\end{aligned}$$

where

$$I_4=\int_0^1\left(1-\tau^2\right)^{\frac{\alpha}{\pi}}\left(t_0^2-\tau^2\right)^{-\frac{1}{2}}\tau^{1-2\frac{\alpha}{\pi}}\,d\tau.$$

Then

$$\begin{aligned}
-\log\frac{dz}{dw} &= -\left(1-\frac{2\alpha}{\pi}\right)\log\left(\frac{1}{t}\sqrt{\frac{t_0^2-t^2}{t_0^2-1}}+\frac{t_0}{t}\sqrt{\frac{1-t^2}{t_0^2-1}}\right)-i\left(\frac{\pi}{2}-\alpha\right)+\log V_\gamma,\\
\frac{dz}{dw} &= \frac{e^{i\left(\frac{\pi}{2}-\alpha\right)}}{V_\gamma}\left(\frac{1}{t}\sqrt{\frac{t_0^2-t^2}{t_0^2-1}}+\frac{t_0}{t}\sqrt{\frac{1-t^2}{t_0^2-1}}\right)^{1-\frac{2\alpha}{\pi}},\\
\frac{dz}{dt} &= \frac{dz}{dw}\cdot\frac{dw}{dt}=\frac{iK}{V_\gamma}\left(\sqrt{\frac{t_0^2-t^2}{t_0^2-1}}+t_0\sqrt{\frac{1-t^2}{t_0^2-1}}\right)^{1-\frac{2\alpha}{\pi}}\left(1-t^2\right)^{\frac{\alpha}{\pi}}\left(t_0^2-t^2\right)^{-\frac{1}{2}}.
\end{aligned}$$

As in the previous sections the constant K is determined from the relation $\int_0^1\frac{dz}{idt}=1:$

$$\begin{aligned}
1 &= \frac{K}{V_\gamma}\int_0^1\left(\sqrt{\frac{t_0^2-t^2}{t_0^2-1}}+t_0\sqrt{\frac{1-t^2}{t_0^2-1}}\right)^{1-\frac{2\alpha}{\pi}}\left(1-t^2\right)^{\frac{\alpha}{\pi}}\left(t_0^2-t^2\right)^{-\frac{1}{2}}\,dt,\\
K &= \frac{V_\gamma}{I_5},
\end{aligned}$$

where

$$I_5 = \int_0^1 \left(\sqrt{\frac{t_0^2 - t^2}{t_0^2 - 1}} + t_0 \sqrt{\frac{1 - t^2}{t_0^2 - 1}} \right)^{1 - \frac{2\alpha}{\pi}} \left(1 - t^2\right)^{\frac{\alpha}{\pi}} \left(t_0^2 - t^2\right)^{-\frac{1}{2}} dt.$$

The conformal representation of the left half Ω_γ is given by

$$z(t) = \frac{K}{V_\gamma} \int_0^t \left(\sqrt{\frac{t_0^2 - \tau^2}{t_0^2 - 1}} + t_0 \sqrt{\frac{1 - \tau^2}{t_0^2 - 1}} \right)^{1 - \frac{2\alpha}{\pi}} \left(1 - \tau^2\right)^{\frac{\alpha}{\pi}} \left(t_0^2 - \tau^2\right)^{-\frac{1}{2}} d\tau.$$

10. The efficiency in the Riabouchinsky model

In the modified Riabouchinsky model the efficiency $\mathcal{E}$ defined by (9) is computed exactly the same way as in Section 7

$$\begin{aligned}
\mathcal{E} &= \frac{P}{P_\infty} = \frac{1}{2} \int_{-1}^{1} V_x \left(V_\gamma^2 - V^2\right) dy = \\
&= \int_0^1 V_x (V_\gamma^2 - V^2)\, dy = \\
&= \int_0^1 \left(\mathrm{Re}\frac{dw}{dz}\right) \left(V_\gamma^2 - V^2\right) dy = \\
&= \frac{1}{i} \int \left(\mathrm{Re}\frac{dw}{dz}\right) \left(V_\gamma^2 - V^2\right) \frac{dz}{dt}\, dt = \\
&= sV_\gamma^2 - \frac{1}{i} \int_0^1 \left(\mathrm{Re}\frac{dw}{dz}\right) \left|\frac{dw}{dz}\right|^2 \frac{dz}{idt}\, dt = \\
&= sV_\gamma^2 - \sin\alpha \int_0^1 \left|\frac{dw}{dz}\right|^3 \frac{dz}{idt}\, dt = \\
&= sV_\gamma^2 - \sin\alpha \frac{V_\gamma^3}{I_5} I_6 = \frac{V_\gamma^3}{I_5} \sin\alpha \left(I_4 - I_6\right),
\end{aligned}$$

where

$$I_6 = \int_0^1 \left(\sqrt{\frac{t_0^2 - t^2}{t_0^2 - 1}} + t_0 \sqrt{\frac{1 - t^2}{t_0^2 - 1}} \right)^{\frac{4\alpha}{\pi} - 2} \left(1 - t^2\right)^{\frac{\alpha}{\pi}} \left(t_0^2 - t^2\right)^{-\frac{1}{2}} t^{3 - \frac{6\alpha}{\pi}} dt.$$

11. Computations

The results of the numerical evaluation of the efficiency for σ in the range from 0.01 to 0.10 are presented in Table 2. For any value of σ the maximum efficiency is attained at the same value of the inclination angle $\alpha = \dfrac{3\pi}{8}$ and increases as σ increases.

Table 2

Inclination angle, α	Cavitation number, σ									
	0.01	0.02	0.03	0.04	0.05	0.06	0.07	0.08	0.09	0.10
0.0000	0.0000	0.0000	0.0000	0.0000	0.0000	0.0000	0.0000	0.0000	0.0000	0.0000
0.0785	0.0178	0.0181	0.0184	0.0186	0.0189	0.0192	0.0194	0.0197	0.0200	0.0203
0.1570	0.0370	0.0375	0.0381	0.0386	0.0392	0.0397	0.0403	0.0409	0.0414	0.0420
0.2356	0.0573	0.0582	0.0590	0.0599	0.0607	0.0616	0.0625	0.0634	0.0642	0.0651
0.3141	0.0788	0.0800	0.0812	0.0824	0.0836	0.0847	0.0859	0.0871	0.0883	0.0896
0.3927	0.1014	0.1029	0.1045	0.1060	0.1075	0.1090	0.1106	0.1121	0.1137	0.1152
0.4712	0.1250	0.1269	0.1287	0.1306	0.1325	0.1344	0.1363	0.1382	0.1401	0.1420
0.5497	0.1493	0.1516	0.1538	0.1560	0.1583	0.1605	0.1628	0.1651	0.1674	0.1697
0.6283	0.1742	0.1768	0.1794	0.1820	0.1846	0.1872	0.1899	0.1925	0.1952	0.1979
0.7068	0.1991	0.2021	0.2051	0.2081	0.2111	0.2141	0.2171	0.2202	0.2232	0.2263
0.7854	0.2238	0.2271	0.2304	0.2338	0.2372	0.2406	0.2440	0.2474	0.2508	0.2543
0.8639	0.2473	0.2510	0.2547	0.2584	0.2622	0.2659	0.2697	0.2735	0.2773	0.2811
0.9424	0.2689	0.2729	0.2769	0.2810	0.2850	0.2891	0.2932	0.2973	0.3015	0.3056
1.0210	0.2871	0.2914	0.2957	0.3000	0.3044	0.3088	0.3132	0.3176	0.3220	0.3265
1.0995	0.3002	0.3047	0.3092	0.3138	0.3183	0.3229	0.3276	0.3322	0.3369	0.3416
1.1781	0.3056	0.3102	0.3148	0.3195	0.3242	0.3289	0.3337	0.3385	0.3433	0.3482
1.2566	0.2996	0.3041	0.3087	0.3133	0.3180	0.3227	0.3275	0.3323	0.3372	0.3422
1.3351	0.2768	0.2811	0.2854	0.2898	0.2942	0.2988	0.3035	0.3082	0.3131	0.3180
1.4137	0.2291	0.2328	0.2366	0.2405	0.2447	0.2490	0.2534	0.2580	0.2628	0.2678
1.4922	0.1439	0.1467	0.1499	0.1536	0.1577	0.1622	0.1671	0.1724	0.1780	0.1839
1.5708	0.0000	0.0000	0.0000	0.0000	0.0000	0.0000	0.0000	0.0000	0.0000	0.0000

12. Concluding remarks

1. As shown above, the the well-known Kirchhoff and Riabouchinsky wake flows can be generalized for the case of partially penetrable obstacles. There exist explicitly solvable situations among them and the explicit solutions are constructed by means of the Kirchhoff method as in the corresponing classical situations. Although the models considered in this paper are rather approximate for immediate practical application, their results are in rather good agreement with experimental data.

2. Some other more exact and complicated models of this type may also be useful engineers working on free flow turbines allowing them to investigate the efficiency limits of the turbines specific types, e.g. cross-flow versus propeller, etc. In most of the situations explicit solvability can hardly be expected; nevertheless they can be investigated by modern numeric methods (variational for example) making them also interesting from the theoretical point of view.

The author is very grateful to Prof. A.M. Gorlov (MIME Dept., Northeastren University, Boston MA USA) whose outstanding achievements in the free flow turbine technology initiated this study and Prof. A.N. Gorban' (Institute of Computational Modeling, Krasnoyarsk, Russia) and Prof. A.S. Demidov (Moscow State University, Moscow, Russia) for helpful discussion.

References

[1] Gorlov A.M. The Helical turbine: a new idea for low-head hydropower // Hydro Review. 1995. Vol. 14, N 5. P. 44–50.

[2] Gorlov A.M. Helical turbines for the Gulf Stream // Marine Technology. 1998. Vol. 35, N 3. P. 175–182.

[3] Gorban' A.N., Gorlov A.M., and Silantyev V.M. Limits of the turbine efficiency for free fluid flow // ASME J. of Energy Resources Technology. 2001. Vol. 123, N 4. P. 311–317.

[4] Milne-Thomson L.M. Theoretical Hydrodynamics. N. Y.: Macmillan, 1960. 632 p.

[5] Lavrentiev M.A., Shabat B.V. Problemy Gidrodinamiki i ikh Matematicheskie Modeli (Problems of hydrodynamics and their mathematical models). M.: Nauka, 1977.

[6] Braverman M., Gorban' A., Silantyev V. Modified Kirchhoff flow with partially penetrable obstacle and its apllication to the the efficiency of free flow turbines // Math. Comput. Modelling. 2002. Vol. 35, N 13. P. 1371–1375.

[7] Demidov A. S. Some applications of the Helmholtz-Kirchhoff method (equilibrium plasma in tokamaks, Hele-Shaw flow, and high-frequency asymptotics) // Russ. J. Math. Phys. 2000. Vol. 7, N 2. P. 166–186.

[8] Friedman A. Variational Principles and Free-boundary Problems. Malabar, FL: R.E. Krieger Publ. Co., Inc., 1988.

[9] Gorban' A., Silantyev V. Riabouchinsky flow with a partially penetrable obstacle // Math. Comput. Modelling. 2002. Vol. 35, N 13. P. 1365–1370.

Received for publication September 1, 2003